Defense Technical Information Center Compilation Part Notice

ADP023900

TITLE: Maneuvering Simulation of Sea Fighter Using a Fast Nonlinear Time Domain Technique

DISTRIBUTION: Approved for public release; distribution is unlimited.

This paper is part of the following report:

TITLE: International Conference on Numerical Ship Hydrodynamics [9th] held in Ann Arbor, Michigan, on August 5-8, 2007

To order the complete compilation report, use: ADA495720

The component part is provided here to allow users access to individually authored sections of proceedings, annals, symposia, etc. However, the component should be considered within the context of the overall compilation report and not as a stand-alone technical report.

The following component part numbers comprise the compilation report:
ADP023882 thru ADP023941

Maneuvering Simulation of Sea Fighter Using A Fast Nonlinear Time Domain Technique

David E. Hess[1], William E. Faller[2], Lisa Minnick[1], and Thomas C. Fu[1]

([1]Naval Surface Warfare Center, Carderock Division,
[2]Applied Simulation Technologies)

ABSTRACT

Efforts to develop and mature a nonlinear time domain technique, based on a fast recursive neural network approach, to simulate the six degree-of-freedom (6-dof) motion of a ship in wind and waves are continuing. Here we describe work to develop a simulation for the Office of Naval Research (ONR) high speed experimental vessel, *Sea Fighter* (FSF-1). Results are presented comparing the measured 6-dof response of *Sea Fighter* operating at sea in sea states 4 & 5 with simulation predictions. The results show that open loop predictions of speed, pitch, heading and trajectory are quite accurate. The predictions for the very small roll angles are not as good indicating that improvements are still needed. Nevertheless, these early results demonstrate an emerging capability for predicting 6-dof ship motions for full scale vehicles in irregular waves.

INTRODUCTION

This work builds upon previous nascent efforts to simulate a model ship operating in large-amplitude regular waves, (Hess, et al., 2006b). In contrast to that effort, the current full scale vehicle has a catamaran hull design, is equipped with water jets versus propellers and is operating in a random wave field. The modeling challenges posed by these differences are discussed. A key element of the approach is a Recursive Neural Network (RNN) which serves as the rapid response ship simulation engine. Experimental time history data required to train the RNN were acquired on *Sea Fighter* during the Rough Water Trial conducted in April, 2006, (Bachman and Powell, 2006). The data include 6-dof ship trajectory, motions and rates from onboard gyros and a GPS compass unit. Also measured were relative wind speed and direction. Critical to the modeling effort is the extensive amount of data on the ambient wave field around the vessel that was also acquired. These data include wave amplitude, wavelength and direction obtained from buoys as well as with the Wave Monitoring System (WaMoS)

and ultrasonic wave height sensors. Results comparing the 6-dof measured response of *Sea Fighter* operating in sea states 4 & 5 are presented and compared with simulation predictions. A successful faster-than-real-time simulation capability in waves will lead to advanced control strategies such as predictive control and path planning as well as the development of virtual sensor systems for real-time analytic redundancy of sensor readings utilized by control systems, (Faller, et al. 2007). A successful simulation of the baseline vehicle can also be used to examine the potential impact that design changes to the vehicle can have on maneuvering, (Faller, et al. 2005, 2006).

Sea Fighter is a high-speed experimental vessel, developed by the Office of Naval Research, and is shown below in Fig. 1. Christened in 2005, she is an aluminum catamaran with two 5500 HP diesel engines and two gas turbines rated at 34 kHP. The vehicle has a length of 262 ft, a beam of 72 ft and a draft of only 11.5 ft, displacing 960 metric tons. The *Sea Fighter* has four steerable Kamewa water jets. Additionally, the *Sea Fighter* has an installed *science package* of strain gauges, accelerometers, pressure gauges, and underwater viewing windows.
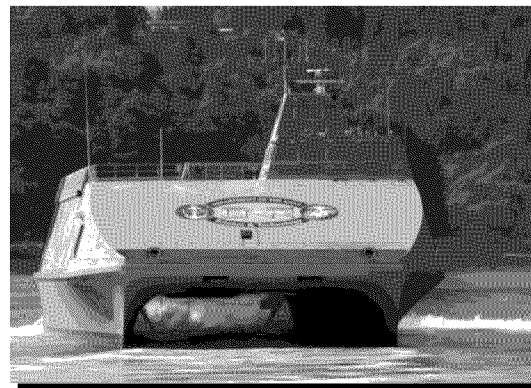

Figure 1. ONR, *Sea Fighter* (FSF-1).

The purpose of the rough water trial was to obtain full-scale qualitative and quantitative hydrodynamic data of a high-speed naval multi-hull in high sea states for CFD tool development and validation. Of primary interest were data associated with slamming events, including forces, motions, and measurement of the impacting wave and ambient conditions (Fu, et al., 2007). The trial took place off of the California coast with the ship traveling at speeds varying from 20-40 kn. The ship's course was varied in order to collect data at multiple headings relative to the ambient wave field. Near field wave data were measured by ultrasonic wave height sensors and the LIDAR system deployed off of the bow, and the WaMoS radar system provided wave information out to 1 nm. The substantial amount of data documenting the 6-dof state of the vehicle as well as the ambient wind and wave conditions makes this an ideal data set for further developing and training the neural network based simulation capability.

The next section will provide some details of the trial and will describe the data that were collected. A substantial amount of effort was required to combine the data from the various systems, synchronize the data to a common time base and prepare it for use as training data. These details are described next.

DATA PROCESSING

The *Sea Fighter* was tested 18-21 April 2006 during a transit from Port Angeles, WA to San Diego, CA. Figure 2 shows a rough sketch of the course taken during the trial. The half circle and irregular path shown south of the Oregon/California border was conducted for the purpose of collecting maneuvering data at a variety of headings to the local wave field. Figure 3 shows a more detailed plot of the maneuvering portion of the trial. The blue line represents the course and is essentially comprised of twelve legs, each at a different heading to the waves. The vehicle spent a substantial amount of time on each leg; to reduce the size of the resulting training data files, shorter segments were removed from each leg. The red sections superimposed on each leg denote the part of the course from which data was extracted. In total, data for twenty-four controlled heading maneuvers, two for each leg, were compiled. Ten of the runs were at 10 m/s (20 kn), ten were at 20 m/s (40 kn), two were at 1.5 m/s (3 kn) and two were at 3 m/s (6 kn). Table 1 provides the segment numbers marked in Figure 3 and the corresponding run numbers.

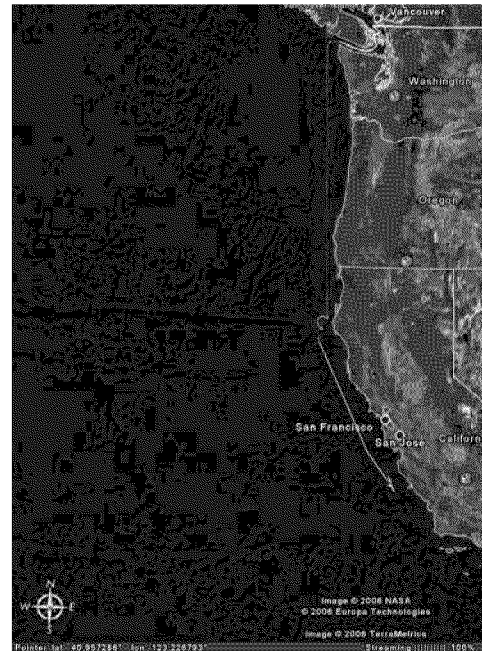The maneuvering data were compiled from three separate sources. A combined GPS and inertial

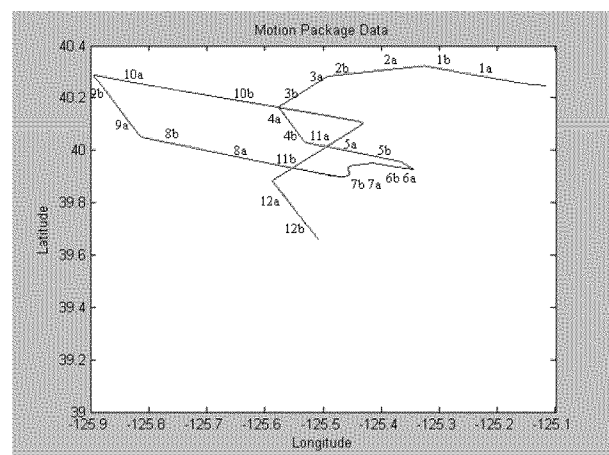
Figure 2. *Sea Fighter* course during April 2006 trial.

Figure 3. *Sea Fighter maneuvering course.*

motion package as well as three Litton LN200s were on board to record the ship's motions. Ship maneuvering data and water jet data were recorded by onboard instruments. In addition, wave height data were collected by a shipboard TSK Wave Height Meter, where TSK refers to the Japanese manufacturer, Tsurumi-Seiki, Co. The TSK system is a motion-compensated microwave CW Doppler radar system, which uses a coherent continuous wave waveform to measure the Doppler shift caused by the velocity of the sea surface relative to the radar. The systems and channels documenting ship motions are discussed next.

Table 1. Segments and corresponding run numbers.

Segment	Run #	Segment	Run #
1a	125a	7a	132a
1b	125b	7b	132b
2a	126a	8a	135a
2b	126b	8b	135b
3a	127a	9a	136a
3b	127b	9b	136b
4a	128a	10a	137a
4b	128b	10b	137b
5a	129a	11a	138a
5b	129b	11b	138b
6a	130a	12a	139a
6b	130b	12b	139b

Ship Motions

Combined GPS and Inertial Motion Package

The combined motion package was installed near the vessel centerline and slightly aft of the second forward-most watertight bulkhead as shown in Figure 5. The motion package consisted of a gyro enhanced orientation sensor (3DM-GX1), a SUPERSTAR II GPS, and a Persistor CF2 CPU. The 3DM-GX1 sensor consists of three angular rate gyros, three orthogonal DC accelerometers, three orthogonal magnetometers, and a multiplexer. The gyros track dynamic orientation while the accelerometers and magnetometers track static orientation. The 3DM-GX1 combines the static and dynamic responses in real time and records 20 samples per second. The SUPERSTAR II GPS provides position, velocity, and time data once every second. The CF2 runs on battery power and combines and stores the collected data on a flash disk. A complete list of the data recorded by this package is provided in Table 2.

The longitude and latitude outputs from the combined GPS/Motion Package are used to track the ship's course as shown in Figure 3. For use in the simulation these outputs needed to be translated into x and y distances measured from an inertial coordinate system. The origin of this system was set at the free surface at a position given by $-125.1°$ longitude and $39.6°$ latitude, which is the lower right hand corner of the plot shown in Figure 3. These outputs were translated into x and y displacements using Eqs. 1 and 2. The conversions from degrees latitude/longitude are based on the recorded latitude and longitude location of the ship.

$$x(m) = (long - long_0) \cdot 85{,}274.88 \, m/long \quad (1)$$

$$y(m) = (lat - lat_0) \cdot 111{,}317.15 \, m/lat \quad (2)$$

Using this definition, a positive x distance is defined to the east, y is positive southward, and z is positive downward into the earth, as shown in Figure 4.
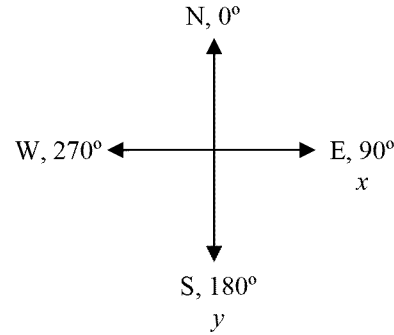

Figure 4. Course coordinate system.

LN 200

Three Litton LN200s were installed aboard the *Sea Fighter*. Each LN200 is an inertial measurement unit consisting of three fiber optic gyros and three linear accelerometers. Table 2 provides a complete list of the data collected by these packages. An LN200 was mounted in the bow of each hull (port and starboard) along the hull's centerline and the third package was mounted in the Mission Bay starboard of the vessel centerline as shown in Figure 5. This allowed for the motion of each hull and that of the overall ship to be examined and compared. The three LN200 inertial motion units provided linear and angular accelerations, angular rates, roll, pitch, and heading data all taken at a sampling rate of 200 Hz. The third LN200 was used to compile the maneuvering data because it is located closest to the vessel centerline and CG. The coordinate system of the unit coincides with the ship coordinate system and is shown in Figure 5; x is positive towards the bow, y is positive starboard, and z is positive downward.

The LN200 directly measures roll and pitch motions, but yaw was calculated from the LN200 heading data. The heading data is based on a coordinate system where 0 degrees is aligned with true north. To calculate yaw, in terms of the ship coordinate system shown in Figure 5, Eq. 3 was used.

$$Yaw = Heading - 90° \quad (3)$$

Water Jet Data

The *Sea Fighter* is equipped with four steerable Kamewa water jets. Shipboard instruments provided water jet data, RPM and nozzle angle, throughout the trial. A zero degree nozzle angle corresponds to a position where the water jets are

parallel with the vessel centerline. A positive nozzle angle corresponds with a starboard turn when the nozzle is deflected starboard.
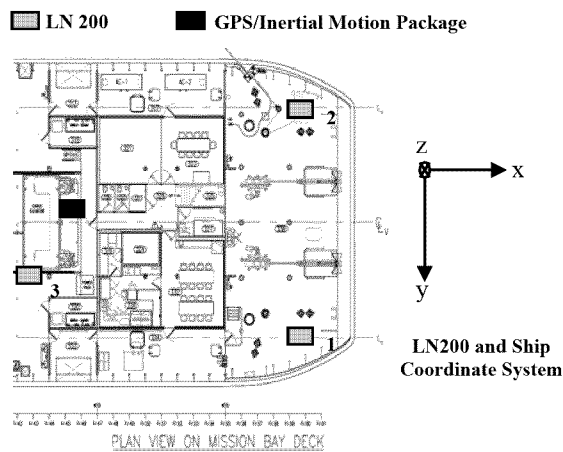

Figure 5. Locations of ship motion packages.

Table 2. Summary of data collected by LN200 and GPS/Inertial motion package.

	LN200	GPS/Inertial Package
Heading	√	
Pitch	√	√
Roll	√	√
Yaw	√	√
X Linear Acceleration	√	√
Y Linear Acceleration	√	√
Z Linear Acceleration	√	√
X Angular Acceleration	√	
Y Angular Acceleration	√	
Z Angular Acceleration	√	
X Angular Rate	√	√
Y Angular Rate	√	√
Z Angular Rate	√	√
Latitude		√
Longitude		√
Altitude		√
Ground Speed		√
Track Angle		√
N. Velocity		√
E. Velocity		√
V. Velocity		√
Date		√
Time		√

TSK Shipborn Wave Height Meter

Wave height data were collected by a TSK wave height meter, which is a shipboard instrument designed to measure wave heights and periods. The system consists of a sensor unit, accelerometer, connections box, and a signal processor. The sensor is mounted directly above the waves to be measured and uses microwaves to detect its target. It has a wave height range of ±14.5 m, resolution of 1.4 cm, a period range of 0 to 20 seconds, and its data includes a Doppler shift due to the sea surface motion. The accelerometer removes ship motion from the amplitude measurements and the signal processor converts the raw data it receives from the connections box into a useable form. It integrates the Doppler motion data to obtain wave amplitude data and then integrates the accelerometer data twice to determine vertical ship motion. The ship motion is then subtracted from the processed sensor data to determine the actual wave amplitude.

Motion & Maneuvering Data Synchronization

Since data was collected from a variety of instruments, each with their own sampling rate, all of the data had to be synchronized. Therefore, the data were all converted to a common 20 Hz sampling rate. This was accomplished by reading in each original set of data and curve fitting the data using a spline fit or linear interpolation to produce 20 data points for every second of data. Table 3 provides a summary of compiled maneuvering data and lists the instrument that provided the data.

This final set of collated data was then passed through a series of FORTRAN codes to accomplish the following steps:

- Fix yaw to remove 2π transitions. (Allows yaw to be differentiated.)
- Derive any missing variables. (Includes differentiation and transformation from inertial to moving coordinate system attached to the ship.)
- Perform a spectral analysis of all variables to determine filter cutoff frequencies.
- Low-pass filter all variables to remove noise. (Use non-recursive digital filters in software.)
- Verify mathematical consistency of all variables.
- Write output files to be read by neural network codes.

Table 3. Summary of maneuvering data and sources.

Roll	LN 200
Pitch	LN 200
Yaw	derived from LN 200 Heading
X Linear Accel	LN 200
Y Linear Accel	LN 200
Z Linear Accel	LN 200
X Angular Rate	LN 200
Y Angular Rate	LN 200
Z Angular Rate	LN 200
X Angular Accel	LN 200
Y Angular Accel	LN 200
Z Angular Accel	LN 200
Heading	LN 200
Wave Height	TSK Wave Height Meter
X	derived from Motion Package/GPS longitude
Y	derived from Motion Package/GPS latitude
Z	Motion Package/GPS
Speed	Motion Package/GPS
Nozzle Angles	Water Jet data
RPM	Water Jet data

DESCRIPTION OF THE SIMULATION

The nonlinear time domain simulation employs a recursive neural network as a computational technique for developing time-dependent nonlinear equation systems that relate input control variables to output state variables. A diagram indicating the various components of the simulation approach is given in Figure 6.

A recursive network is one that employs feedback; namely, the information stream issuing from the outputs is redirected to form additional inputs to the network. The RNN is used to predict the time histories of maneuvering variables of Sea Fighter conducting maneuvers in sea states 4 & 5 at a variety of wave encounter angles. These maneuvers have been used to train and validate the neural network. Upon completion of training, data from maneuvers not included in the set of training maneuvers are input into the simulation, and predictions of the motion of the vehicle are obtained. The input data required for the vehicle consists of time histories of the control variables: jet speed (measured by RPM), nozzle angles, port and starboard skeg angles, along with the initial conditions of the vehicle at some prescribed starting location. As the simulation proceeds, these inputs are combined with past-predicted values of the outputs to estimate the forces and moments that are acting on the vehicle. The resulting outputs are predictions of the time histories of the state variables: linear and angular velocity components, which can then be integrated to obtain trajectory and attitude, and differentiated to recover the accelerations acting on the vehicle.

The specification of the wave field: heading angle, frequency and amplitude for each component must be provided. Input forces and moments using these quantities have been implemented. Thus, the neural network uses forces and moments acting on the vehicle (both from the controls and from the environment) and translates it into vehicle motion. Predictions of such variables as trajectory components, speed, heading, roll and pitch will be provided in the results section.
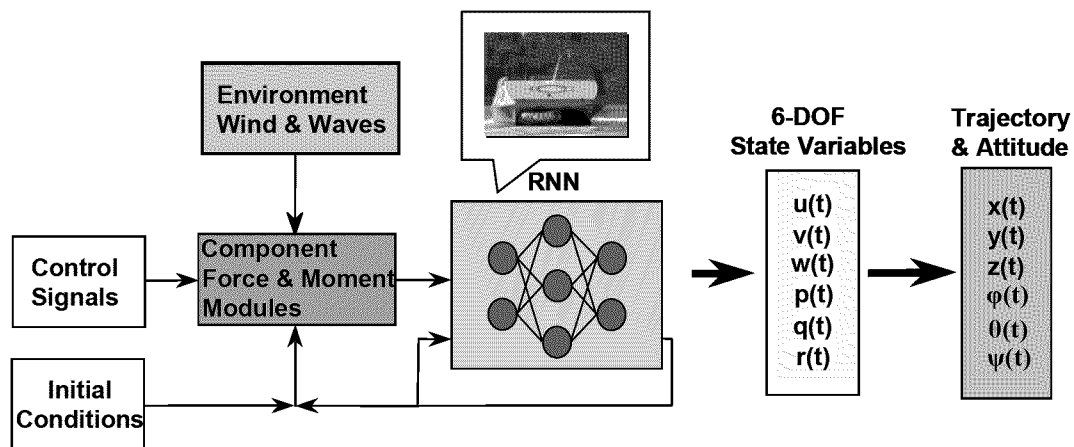

Figure 6. Schematic of Simulation Technique

The architecture of the recursive neural network is illustrated schematically in Figure 7. The network consists of four layers: an input layer, two *hidden* layers and an output layer. Within each layer are nodes, which contain a nonlinear transfer function
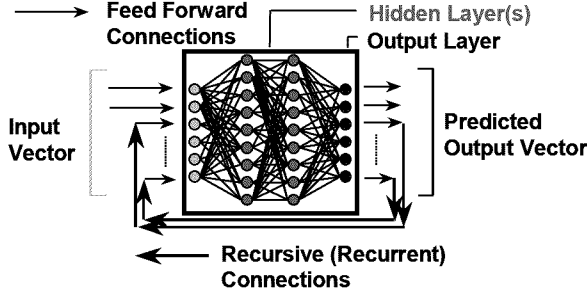

Figure 7. Recursive neural network.

that operates on the input to the node and produces a smoothly varying output. The binary sigmoid function was used for this work; for input x ranging from $-\infty$ to ∞, it produces the output y which varies from 0 to 1 and is defined by

$$y(x) = \frac{1}{1+e^{-x}} \quad . \tag{4}$$

Note that the nodes in the input layer simply serve as a means to couple the inputs to the network; no computations are performed within these nodes. The nodes in each layer are fully connected to those in the next layer by weighted links. As data travels along a link to a node in the next layer it is multiplied by the weight associated with that link. The weighted data on all links terminating at a given node is then summed and forms the input to the transfer function within that node. The output of the transfer function then travels along multiple links to all the nodes in the next layer, and so on. So, as shown in Figure 7, an input vector at a given time step travels from left to right through the network where it is operated on many times before it finally produces an output vector on the output side of the network. Not shown in Figure 7 is the fact that most nodes have a bias; this is implemented in the form of an extra weighted link to the node. The input to the bias link is the constant 1 which is multiplied by the weight associated with the link and then summed along with the other inputs to the node. For further details concerning the operation of neural networks, the reader is directed to (Haykin, 1994), and for recursive neural networks to (Faller, *et al.*, 1997).

A recursive neural network has feedback; the output vector is used as additional inputs to the network at the next time step. For the first time step,

when no outputs are available, these inputs are filled with initial conditions. The time step at each iteration represents a step in dimensionless time, $\Delta t'$. Time is rendered dimensionless using the ship's length and its speed computed from the preceding iteration; thus, the dimensionless time step represents a fraction of the time required for the flow to travel the length of the hull. The neural network is stepped at a constant rate in dimensionless time through each maneuver. Thus, an input vector at the dimensionless time, t', produces the output vector at $t' + \Delta t'$, where

$$t' + \Delta t' = t' + \frac{\Delta t\, U(t')}{L} \quad \text{and} \quad \Delta t' = 0.07 \quad . \tag{5}$$

Because ship speed, $U(t')$, varies while length, L, is constant, the spacing between samples, Δt, must vary in order that the dimensionless time step, $\Delta t'$, remain constant at the chosen value of 0.07.

The recursive neural network described here has 91 inputs for maneuvers in waves. Each hidden layer contains 74 nodes, and each of these nodes uses a bias. The output layer consists of 6 nodes, and does not use bias units. The network contains 154 computational nodes and a total of 12,802 weights and biases. The input vector, described in detail below, consists of a series of forces and moments which act on the vehicle, and the network then predicts at each time step dimensionless forms of the six state variables: three linear velocity components u, v, and w, and three angular velocity components p, q and r. Specifically, the outputs are defined as

$$u'(t' + \Delta t') = \frac{u(t' + \Delta t')}{U(t')}, \quad v' \text{ and } w' \text{ similar}$$
$$p'(t' + \Delta t') = \frac{p(t' + \Delta t')\, L}{U(t')}, \quad q' \text{ and } r' \text{ similar} \tag{6}$$

These velocity predictions are then used to compute, at each time step, the remaining kinematic variables: trajectory components, Euler angles (attitude) and accelerations.

The contributions that form the input vector are described as follows. Nineteen basic force and moment terms describe the influence of the control inputs and of time-dependent flow field effects. Hull forces and moments are given by X, Y, Z, K, M and N. The axial thrust component from the water jets is considered as two terms, the combined thrust from the starboard side and from the port side, T_{X-star} and T_{X-port}. Because the water jets are steerable, sideways thrust components exist and are denoted as, T_{Y-star}

and T_{Y-port}. Two restoring moments resulting from disturbances in pitch and roll are written as K_r and M_r. Also included are additional moments in roll and pitch that result from roll-pitch coupling, K_{RP} and M_{RP}. For operation in waves, two forces and two moments are added: longitudinal and lateral wave forces and pitch and yaw moments, X_{wave}, Y_{wave}, M_{wave} and N_{wave}. The final input is the wave elevation, δ_{wave}. These input terms are formulated from knowledge of water jet rpm and nozzle angles, geometry of the vehicle, and from output variables which are recursed and made available to the inputs, and from the available wave information. The modules which define the input terms are referred to as component force modules in Figure 6, and a description of these basic inputs is provided in the next section.

Additional inputs are obtained by retaining past values of the basic inputs. This gives the network memory of the force and moment history acting on the vehicle and permits the network to learn of any delay that can occur between the application of the force or moment and the response of the vehicle. For the hull inputs: *X, Y, Z, K, M* and *N*, 4 past values are retained. Two past values from each of the two water jet axial thrust terms and 4 past values from the two sideways thrust components are kept. One past value is kept for each of the restoring moment terms. For the four wave force and moment terms, 4 past values are retained and 4 past values are kept for the wave elevation input. The number of past values to keep is chosen empirically and appears to be a function of the frequency response of the vehicle. For example, retaining information for 4 past values implies the network is given information about past events for a period of time required for the flow about the vehicle to travel 28% of the length of the hull.

Recursed outputs from the prior time step are used as six additional contributions to the input vector. Furthermore, the output vector from one previous time step is retained and made available as six additional inputs. Knowledge of the output velocities for two successive time steps permits the network to implicitly learn about the accelerations of the vehicle. A summary of the various contributions that make up the input vector is provided in Table 4, and attention is next directed to a explanation of the basic force and moment inputs.

Table 4 Summary of network inputs.

Input Description	Inputs
$X(t'), X(t'-\Delta t'), \ldots, X(t'-4\Delta t')$	5
$Y(t'), Y(t'-\Delta t'), \ldots, Y(t'-4\Delta t')$	5
$Z(t'), Z(t'-\Delta t'), \ldots, Z(t'-4\Delta t')$	5
$K(t'), K(t'-\Delta t'), \ldots, K(t'-4\Delta t')$	5
$M(t'), M(t'-\Delta t'), \ldots, M(t'-4\Delta t')$	5
$N(t'), N(t'-\Delta t'), \ldots, N(t'-4\Delta t')$	5
$T_{X-star}(t'), T_{X-star}(t'-\Delta t'), T_{X-star}(t'-2\Delta t')$	3
$T_{X-port}(t'), T_{X-port}(t'-\Delta t'), T_{X-port}(t'-2\Delta t')$	3
$T_{Y-star}(t'), T_{Y-star}(t'-\Delta t'), \ldots, T_{Y-star}(t'-4\Delta t')$	5
$T_{Y-port}(t'), T_{Y-port}(t'-\Delta t'), \ldots, T_{Y-port}(t'-4\Delta t')$	5
$K_r(t'), K_r(t'-\Delta t')$	2
$M_r(t'), M_r(t'-\Delta t')$	2
$K_{RP}(t'), K_{RP}(t'-\Delta t')$	2
$M_{RP}(t'), M_{RP}(t'-\Delta t')$	2
$X_w(t'), X_w(t'-\Delta t'), \ldots, X_w(t'-4\Delta t')$	5
$Y_w(t'), Y_w(t'-\Delta t'), \ldots, Y_w(t'-4\Delta t')$	5
$M_w(t'), M_w(t'-\Delta t'), \ldots, M_w(t'-4\Delta t')$	5
$N_w(t'), N_w(t'-\Delta t'), \ldots, N_w(t'-4\Delta t')$	5
$\delta_w(t'), \delta_w(t'-\Delta t'), \ldots, \delta_w(t'-4\Delta t')$	5
$u'(t'), v'(t'), w'(t'), p'(t'), q'(t'), r'(t')$	6
$u'(t'-\Delta t'), v'(t'-\Delta t'), w'(t'-\Delta t'),$ $p'(t'-\Delta t'), q'(t'-\Delta t'), r'(t'-\Delta t')$	6
Total	91

FORCE AND MOMENT INPUTS

Neural networks have an amazing ability to identify and track nonlinear behavior linking a set of inputs to a set of outputs. This innate ability can be further augmented, however, by carefully constructing physically motivated input and output variables that form a well-posed problem. For this task, inputs to the neural network were cast in the

form of hull forces (X, Y, Z) and moments (K, M, N) acting on the vehicle. This input formulation is more general in the sense that training data may now originate from experiments or from simulations. The total forces and moments are determined by training a set of feedforward neural networks, one for each force or moment component, to predict X, Y, Z, K, M, N from quantities that will be available on the input side of the RNN. Recall that these variables originate from controls, output variables which are recursed and made available to the inputs and from variables which may be derived from these. Examples are: ($n_1, n_2, \zeta_1, \zeta_2, u, v, w, p, q, r, \alpha, \beta, q', r', \ldots$). Six feedforward networks were then developed, and each used a customized set of the inputs listed above. They were trained and prepared for use prior to the development of the RNN. Then, they were implemented as subroutines on the input side of the larger RNN code. The X, Y, Z, K, M, N outputs from the feedforward networks were used as inputs to the RNN at each time step.

These basic hull input terms were augmented by explicit expressions for axial and sideways thrust from the water jets, restoring moments resulting from disturbances in pitch and roll and wave elevation and forces acting on the hull. These terms were fashioned from the control variables: water jet rpm, n_{star} and n_{port}; and nozzle deflection angles: ζ_{star} and ζ_{port}. Also available for the definition of the input terms are output variables from the previous time step, which are recursed and made accessible to the input side of the network. In this manner a true simulation is preserved as only the control histories and initial conditions of the vehicle are required to run the simulation. The following paragraphs describe the creation of each of the input terms.

The axial thrust component is assumed to be related to the advance ratio, $J = U/nD$. To prevent code difficulties if n should drop to zero, the reciprocal of J became the actual input as shown in Eq. 7:

$$T_{X-star} \Rightarrow \frac{1}{J_{star}} \propto \frac{n_{star} \cos \zeta_{star}}{u}$$
$$T_{X-port} \Rightarrow \frac{1}{J_{port}} \propto \frac{n_{port} \cos \zeta_{port}}{u} \qquad (7)$$

Similarly, the sideways thrust components were expressed as:

$$T_{Y-star} \Rightarrow \frac{1}{J_{star}} \propto \frac{n_{star} \sin(a\zeta_{star})}{u}$$
$$T_{Y-port} \Rightarrow \frac{1}{J_{port}} \propto \frac{n_{port} \sin(a\zeta_{port})}{u} \qquad (8)$$

where a is a constant amplification factor designed to magnify the influence of these terms despite often very small nozzle angles.

Righting moment inputs are provided to account for disturbances in roll and pitch. The product of the moment arm and the weight of the vehicle creates a couple which acts to restore the vehicle to its undisturbed orientation. These moments may be approximated by

$$K_r = -\rho \, g \, \nabla \overline{GM_T} \sin \varphi$$
$$M_r = -\rho \, g \, \nabla \overline{GM_L} \sin \theta \qquad (9)$$

where ∇ is volumetric displacement, φ and θ are angles of roll and pitch, and $\overline{GM_T}$ & $\overline{GM_L}$ are the transverse & longitudinal metacenters. The metacentric height is commonly decomposed into a difference between the distance from the center of buoyancy to the metacenter, $\overline{BM_T}$ or $\overline{BM_L}$, and the distance from the center of buoyancy to the center of gravity, $\overline{BG}$. $\overline{BM_T}$ and $\overline{BM_L}$ may be approximated for small roll and pitch motions by I_T/∇ and I_L/∇, where I_T and I_L are moments of inertia of the wetted portion of the vehicle about the transverse or longitudinal centerline, respectively. Upper bounds on these moments for most ships satisfy $I_T < 1/12\,B^3 L$ and $I_L < 1/12\,BL^3$, where B is the beam and L is the overall length of the vehicle. Replacing the fraction with a constant, the restoring moments may then be written as

$$K_r = -\rho \, g \nabla \left(\frac{c_T B^3 L}{\nabla} - \overline{BG} \right) \sin \varphi$$
$$M_r = -\rho \, g \nabla \left(\frac{c_L BL^3}{\nabla} - \overline{BG} \right) \sin \theta \qquad (10)$$

This information, when available, can be explicitly provided; alternatively, the simpler expressions

$$K_r = -C_T \sin \varphi \text{ and } M_r = -C_L \sin \theta \quad (11)$$

may be used, allowing the network to determine the unknown constants.

The additional moments in roll and pitch that result from roll-pitch coupling, K_{RP} and M_{RP} are defined as:

$$K_{RP} = -\rho\, g\, \nabla \overline{GM_T} \sin\varphi \cos\theta \cos\varphi$$
$$M_{RP} = -\rho\, g\, \nabla \overline{GM_L} \sin\theta \cos\theta \cos\varphi \qquad (12)$$

As before, the simpler expressions given in Eq. 13 were used.

$$K_{RP} = -C_T \sin\varphi \cos\theta \cos\varphi$$
$$M_{RP} = -C_L \sin\theta \cos\theta \cos\varphi \qquad (13)$$

The specification of the wave field requires the heading angle, ψ_i, angular frequency, ω_i, and amplitude, A_i, for each of the wave components. This data is used to construct the wave encounter angle, β, the wave number, k, and the wave encounter frequency, ω_e, as given in (Lloyd, 1998):

$$\beta = \psi_{wave} - \psi_{ship}, \quad k_i = \frac{\omega_i^2}{g}$$
$$\text{and } \omega_{ei} = \omega_i - \frac{\omega_i^2}{g} U \cos\beta \qquad (14)$$

Then, the wave elevation, δ_i, and the wave slope, s_i, are computed using:

$$\delta_i(t) = A_i \cos(\omega_{ei} t + \phi_i)$$
$$s_i(t) = A_i k_i \sin(\omega_{ei} t + \phi_i) \qquad (15)$$

and the force components and yawing moment are given (Fossen, 1994) as

$$X_w(t) = \sum_{i=1}^{N} \rho g BLD \cos\beta\, s_i(t),$$
$$Y_w(t) = -\sum_{i=1}^{N} \rho g BLD \sin\beta\, s_i(t)\ .$$
$$M_w(t) = -\sum_{i=1}^{N} \frac{1}{24} \rho g BLD \left(L^2 - B^2\right) k_i^2 \cos(2\beta)\, \delta_i(t)$$
$$N_w(t) = \sum_{i=1}^{N} \frac{1}{24} \rho g BLD \left(L^2 - B^2\right) k_i^2 \sin(2\beta)\, \delta_i(t)$$
$$(16)$$

The subscript i varies over the measured wave components.

The basic inputs to the network have now been defined. They consist of hull forces and moments, axial and sideways thrust components from the waterjets, restoring moments to disturbances in roll and pitch, and wave forces and moments acting on the hull of the vessel along with the wave elevation. The description of the architecture of the neural network is now complete. The training of the network has been carried out in a manner consistent with that described previously, (Hess, *et al.*, 2006a).

The results of these simulations proved to be very encouraging and are detailed next.

RESULTS

The predictions shown here are for the full scale catamaran, *Sea Fighter*, operating in sea states 4 & 5 off of the coast of California. The real-time nonlinear simulation (RNS) results represent time-domain predictions of a surface ship in random seas. All simulations were run open-loop using the water jet RPM and nozzle deflection angles as the control inputs. As such, there is no compensation for simulation error via a feedback controller driving the simulation predictions to match the measured trajectory. The RNS is simply given the open-loop control time-histories and the wave field as specified by amplitude, frequency, and direction, and asked to predict the complete time history of the ship motion in waves. This is a much more difficult task than when an automatic control system is used to drive the simulation. In general, the only way to truly test the fidelity of a simulation is to run the simulation open-loop using measured control inputs and to then compare the resultant predictions directly to the measured response of the physical system as was done here.

A subset of nine of the maneuvers given in Table 1 (125b, 126a, 126b, 127a, 127b, 128a, 128b, 129a and 129b) was used to develop the results. These maneuvers were conducted at a speed of 10 m/s (20 kn) corresponding to a Froude number of 0.15. Of the nine runs, six were used to train the simulation. The other three (126a, 127b, 128a) were set aside to test the ability of the network to make reasonable predictions for maneuvers similar to those in the training set, but not seen during the training. These are denoted validation or novel runs. Because the simulation has no *a priori* knowledge of these maneuvers, they can be used to judge how well the final simulation generalizes to novel conditions. This set of runs comprises a total of 5 different wave encounter angles (37°, 83°, 128°, 173° and 217°), and the validation cases span 3 different wave encounter angles (83°, 128° and 173°). These results represent the first set of predictions for a full scale vehicle in waves in the open ocean operating at multiple wave encounter angles.

The ship is fitted with a pair of skegs that may be operated in a fixed or active mode as described in (Rossignol, 2006). For all of the maneuvers in Table 1, the skegs were maintained in a fixed position with the starboard at -6.8° and the port at -5.5°. The reversing bucket position channels (Griggs, 2007) for each of the four water jets remained at 100% indicating that they did not serve

as controls for any of the maneuvers presented in the results.

During the data preparation phase after the trial had concluded, examination of the four water jet rpm signals revealed that they did not vary over the 24 maneuvers listed in Table 1, although these runs were conducted at four different speeds. As a substitute for this problem, the powering data for *Sea Fighter*, given in (Griggs, 2007), was consulted and used to supply constant rpm values, n_{star} and n_{port}, for each speed. This solution is viable because the maneuvers are conducted at constant speed; however, any small rpm variations due to speed corrections are lost.

Figure 8 shows one of the training files, 128b. In all cases, the commanded control inputs and initial conditions are the only inputs to the simulation and the RNS predicts the ship trajectory, speed, roll, pitch, and heading. These predicted values are then compared directly to the measured data in order to determine the simulation fidelity. The two upper plots are one of the rpm and one of the nozzle angle control signals which reflect the corresponding commanded control inputs to the ship. The next plots, in all cases, are speed, roll, pitch, heading (with the abscissa given as time) and trajectory components, x vs. y. In all graphs the measured data are shown in black, and the RNS predictions in red. For Figure 8, additional plots of the direct outputs of the simulation, three linear velocity components and three angular velocity components, are given.

As can be seen, the trajectory of the vehicle is predicted very accurately with only a minor deviation near the end of the run. Speed, heading, pitch and roll are also recovered very nicely. As these are derived quantities, the level of accuracy is due to the high degree of fidelity in the velocity outputs predicted by the simulation. The fact that the predictions match extremely well to the measured data indicate that the problem is well posed to the recursive neural network, and that the simulation is able to learn the relationships between the input controls and the output states.

Shown in Figures 9-11 are all three of the validation maneuvers. In each case the trajectory is predicted remarkably well over the entire extent of the run with only minor deviations near the end. The speed is recovered almost perfectly, with the exception of the minor fluctuations. The pitch and heading signals show greater deviations, nevertheless the overall nature of the response is predicted accurately. The roll response of the vehicle is very small; the simulation is having the most difficulty

with this behavior. Overall, the results are extremely good and demonstrate that the RNS approach appears to be an effective method for simulating controlled heading maneuvers by *Sea Fighter* in the open ocean.

One of the difficulties presented by this set of data was the type of maneuver itself. By its very nature a controlled heading maneuver, in which the vehicle primarily travels on a straight track at constant speed, is one for which most of the variables besides speed, are very close to zero. This situation is more difficult for the neural network to train to and generalize well. These results show that it can be done. Further, these results are consistent with previous efforts for the prediction of various kinds of ship maneuvers for free-running models operating in controlled conditions in a test basin and for full scale ships operating in the open ocean, (Hess, *et al.*, 2006a, 2006b).

CONCLUSIONS

These early results demonstrate an emerging capability for predicting 6-dof ship motions in both regular and irregular waves. The paper has described further improvements to the RNN surface ship simulation tools and has demonstrated the capability by producing 6-dof predictions of Sea Fighter operating in sea states 4 & 5. The paper, and in particular, the full scale ship data in irregular waves has also pointed out several areas where improvements need to be made.

For Sea Fighter operating in the open ocean, in irregular waves, the phase angle for the wave elevation equation was not known. In model tests, the phase angle can be estimated from the measured depth and the regular wave amplitude, similar methods for estimating the phase angle need to be developed for full scale ships in the open ocean. A better method for determining and representing the real wave elevation and wind conditions also needs to be developed for the RNN simulations in irregular waves. We assumed a single regular wave, dominant swell component, and no wind since this was the only data available from the buoys (one wave frequency, one wave amplitude, one wave direction, and no phase angle). One approach to answering these questions may be to use the ship as a sensor in order to estimate as much as possible about the waves and environmental conditions. Techniques along these lines are being explored for model scale data with known regular wave components and should be explored for full-scale ships in the open ocean.

Overall, while the RNN simulations at full-scale yield good results, it is clear that additional work remains to be done in order to better model the
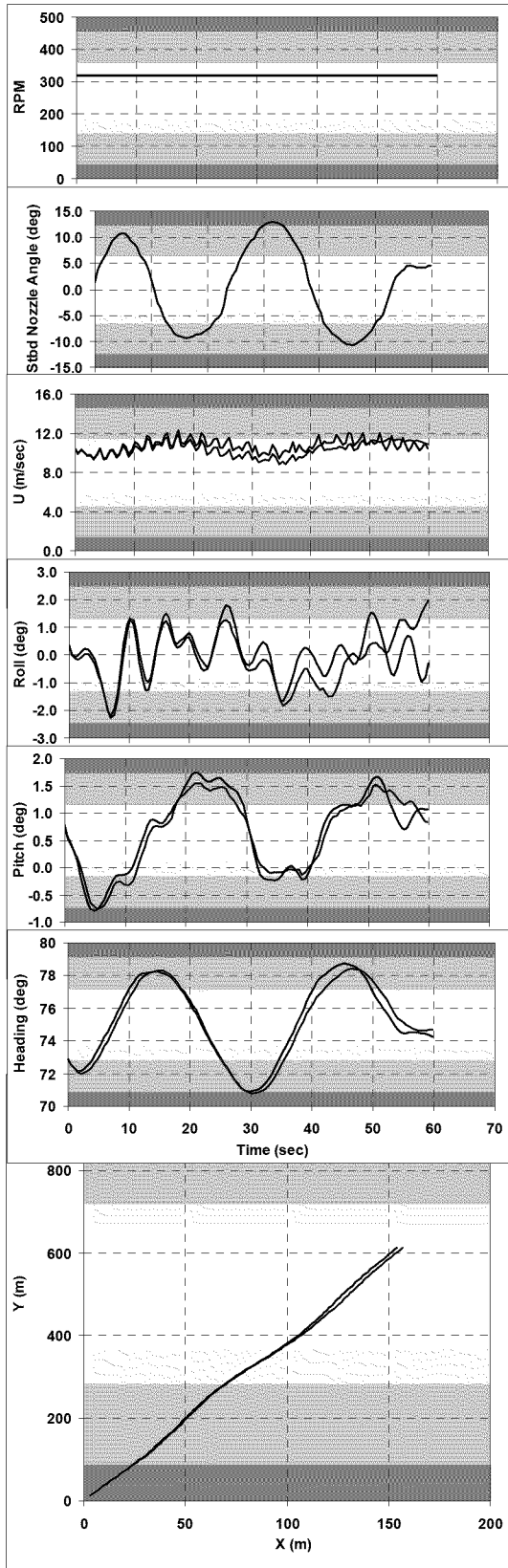
Fig. 8a. Training file 128b
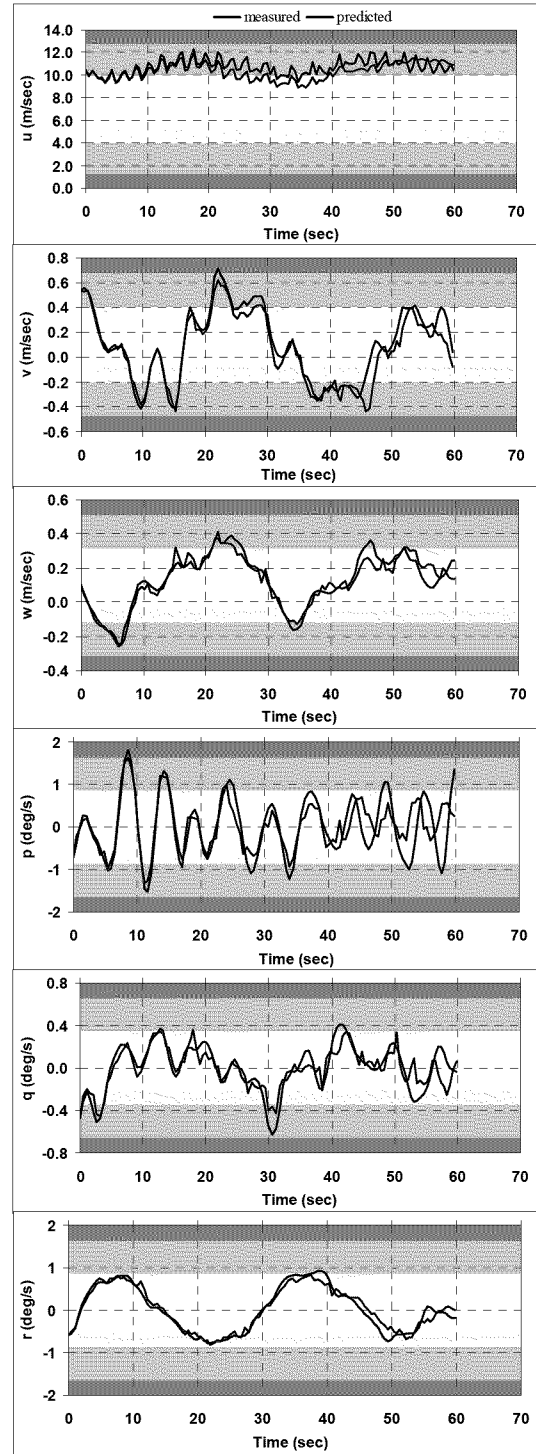Black – Measurements, Red – RNS Predictions

Fig. 8b. Training file 128b
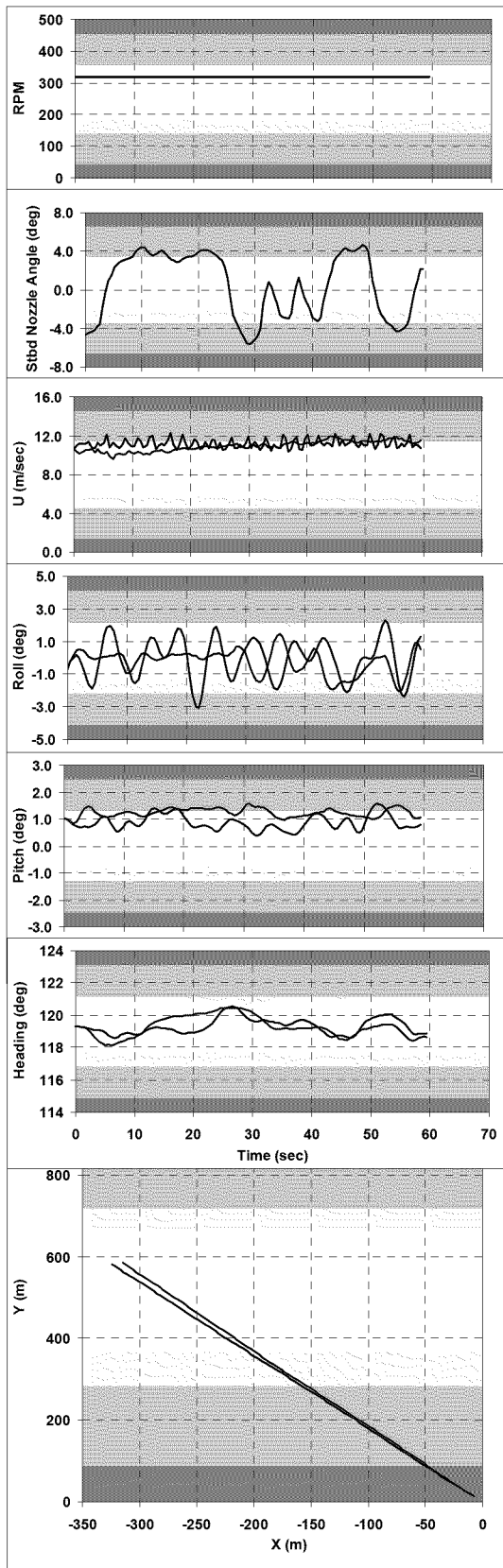Black – Measurements, Red – RNS Predictions

Fig. 9. Validation file 127b
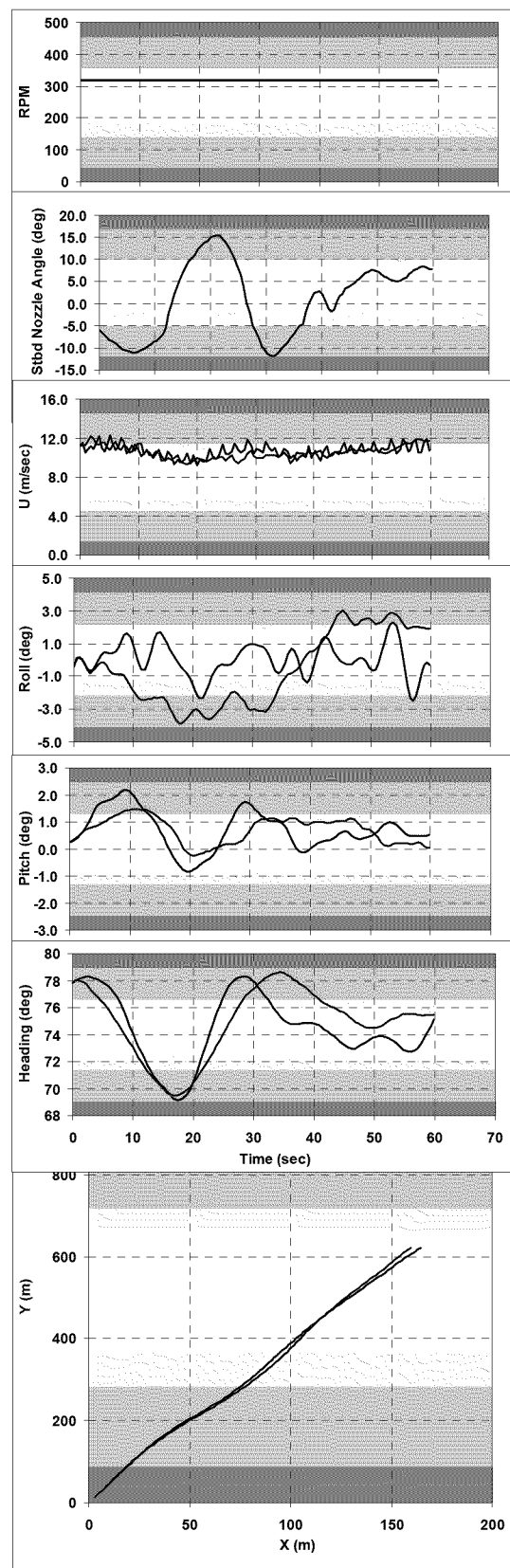Black – Measurements, Red – RNS Predictions

Fig. 10. Validation file 128a
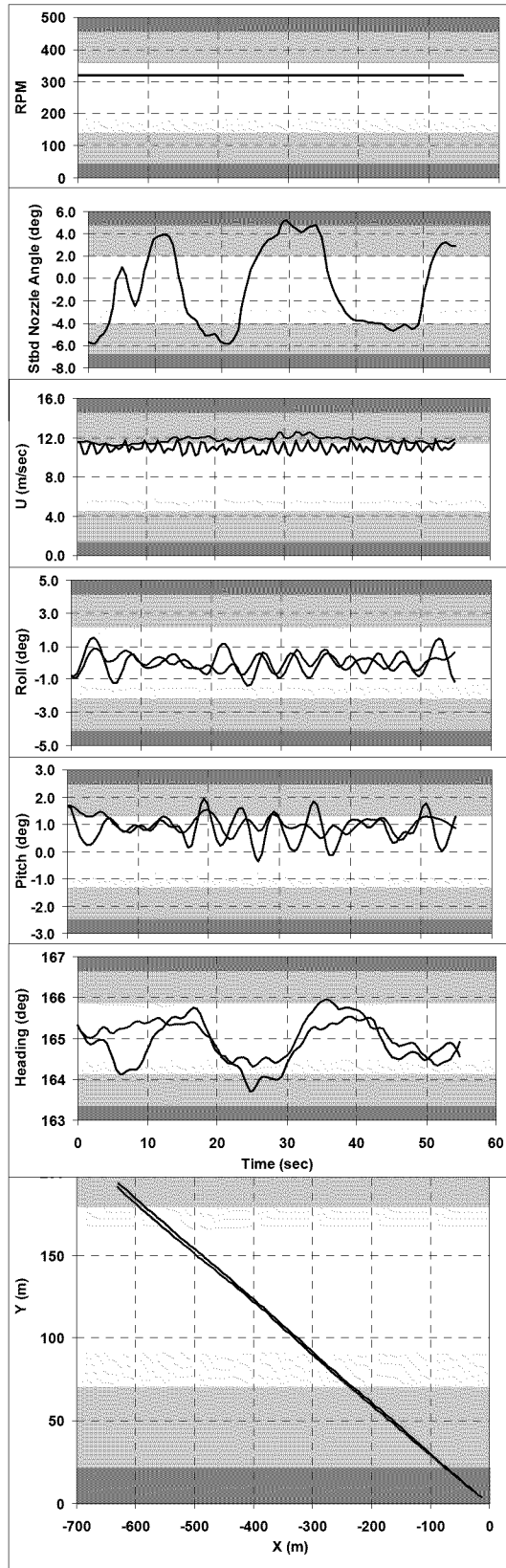Black – Measurements, Red – RNS Predictions

Fig. 11. Validation file 126a
Black – Measurements, Red – RNS Predictions

environmental forcing functions, waves and wind, as well as the corresponding force and moment equations which form the inputs to the RNN simulation. Further, at full-scale, additional data issues exist which must be dealt with. For example, how do you accurately measure or estimate depth/heave? How do you readily determine the wave field being encountered? Clearly, a single frequency and amplitude corresponding to the dominant swell will not be sufficient in most cases.

To summarize, the results demonstrate the capability for predicting 6-dof ship motions at full-scale in sea states 4 & 5 using a nonlinear time domain technique. However, the full scale ship simulations have also pointed out several areas where improvements can and should be made to the RNN simulation approach.

ACKNOWLEGEMENTS

REFERENCES

Bachman, R.J. and M.D. Powell, "Sea Fighter (FSF-1) Seakeeping Measurements Off Pt. Conception," Naval Surface Warfare Center Quick Look Report, (February 2006).

Faller, W.E., Smith, W.E., and Huang, T.T. "Applied Dynamic System Modeling: Six Degree-Of-Freedom Simulation Of Forced Unsteady Maneuvers Using Recursive Neural Networks", 35th AIAA Aerospace Sciences Meeting, Reno, NV, AIAA-97-0336, 1997, pp. 1-46.

Faller, W.E., D.E. Hess and T.C. Fu, "Simulation Based Design: A Real-Time Approach using Recursive Neural Networks," AIAA Paper 2005-911, 43rd AIAA Aerospace Sciences Meeting (January 10-13, 2005), Reno NV, pp. 1-13.

Faller, W.E., D.E. Hess and T.C. Fu, "Real-Time Simulation Based Design Part II: Changes in Hull Geometry," AIAA Paper 2006-1485, 44th AIAA Aerospace Sciences Meeting (January 9-12, 2006), pp. 1-16.

Faller, W.E., D.E. Hess, T.C. Fu and E.S. Ammeen, "Analytic Redundancy for Automatic Control Systems: Recursive Neural Network Based Virtual Sensors," AIAA Paper 2007-156, 45th AIAA Aerospace Sciences Meeting (January 8-11, 2007), Reno NV, pp. 1-18.

Fossen, T.I. Guidance and Control of Ocean Vehicles, Wiley, New York, 1994.

Fu, T.C., A.M. Fullerton and L. Minnick, "Characterization of Sea Fighter, FSF-1, Wave Slam Events." Abstract submitted to the 9th International Conference on Numerical Ship Hydrodynamics (NSH 07), August 5-8, 2007, Ann Arbor, Michigan.

Haykin, S. Neural Networks: A Comprehensive Foundation, Macmillan, New York, 1994.

Griggs, D., "FSF-1 SEA FIGHTER Standardization and Tactical Trials Results," NSWCCD Hydrodynamics Department Technical Report, NSWCCD-50-TR-2007/047, (May 2007), p.14.

Hess, D.E., Faller, W.E., Fu, T.C. and Ammeen, E.S. "Improved Simulation of Ship Maneuvers Using Recursive Neural Networks," 44th AIAA Aerospace Sciences Mtg, Reno, NV, (Jan. 9-12, 2006a), AIAA-2006-1481, pp.1-20.

Hess, D.E., W.E. Faller, J. Lee, T.C. Fu and E.S. Ammeen, "Ship Maneuvering Simulation in Wind and Waves: A Nonlinear Time-Domain Approach Using Recursive Neural Networks," 26th Symposium on Naval Hydrodynamics, Rome, Italy, (September 17-22, 2006b), Preprints Vol. II, pp. 21-38.

Lloyd, A.R.J.M., Seakeeping: Ship Behaviour in Rough Weather, Publisher: A.R.J.M. Lloyd; 2nd Rev. Ed., (May 1, 1998), ISBN:0953263401.

Rossignol, G.A, "Maneuvering Trials Conducted on the High-Speed Catamaran Sea Fighter (FSF 1)," NSWCCD Hydrodynamics Department Technical Report, NSWCCD-50-TR-2006/054, (Dec. 2006).